

Multi-source contamination mapping on the ground: a novel approach

Dor Raz^{1,*}, Ohad Fitoussi², Nadav Ben-David¹, Eran Vax², Alon Osovizky³, Guy Zaidner²

¹Israel Atomic Energy Commission, Israel

²Negev Nuclear Research Center, Israel

³Rotem Industries Ltd, Israel

(*) dra@post.bgu.ac.il

Abstract—Multi-source contamination mapping is a critical aspect of radiation detection and environmental monitoring. This paper introduces an innovative algorithm for accurate and efficient multi-source contamination mapping. The algorithm comprises two main components: (1) search area identification and (2) source localization using a particle filter. The search area identification involves extrapolating directional measurements to create search areas, employing clustering algorithms to refine these areas, and generating final search areas based on weighted factors. The incorporation of directional measurements significantly enhances performance by reducing parameter search space of the particle filter and thus improving practical application potential. The particle filter-based source localization employs a four-stage process, involving generation of initial guesses, comparison of expected and acquired measurements, employing genetic algorithms for particle selection, and a convergence criterion. The algorithm's efficacy is demonstrated through four simulated experimental scenarios, each with varying numbers and densities of point radioactive sources. Results illustrate successful search area identification and source localization with an average error of approximately 1 meter and source activity estimation of within 25% of the ground-truth values. Further improvements to the area clustering algorithm, improved mission planning for online applications, and extensive testing of the algorithm are planned in the future. With these improvements, the algorithm presented here could enhance the ability to respond to radioactive contamination incidents swiftly and effectively, ensure timely mapping of contaminated areas, and maintain human safety in the event of an incident.

Keywords—Particle filter, clustering, mapping, contamination

I. INTRODUCTION

RADIOMETRIC surveys are required for nuclear sites, whether they are active, decommissioned, or scheduled for decommissioning. Inspecting a nuclear site ensures personnel safety, facilitates systematizing the inspection process, allows repeatable monitoring missions, enables access to highly radioactive environments, and makes rapid and comprehensive searches at a low cost possible [1]. The current approach to contamination mapping and decommissioning relies on human operators, which is inefficient, dangerous, and time-consuming [2, 3]. In order

to reduce the exposure of workers to high radiation doses during decommissioning, it is necessary to calculate where radioactive contamination may occur. As a result, it is imperative that technologies be developed and implemented that can inspect sites and detect radiation hot spots [4]. Site inspection generally involves the mapping of radiation and the mapping of space. As a result, a number of approaches to nuclear site inspection have been described in the literature, largely based on ground robots, unmanned aerial vehicles, and underwater robots [1] which are a natural fit for the task.

Decommissioning and post-operational clean-up activities may benefit greatly from high-resolution radiation mapping [5]. Several attempts have been made recently to develop algorithms and platforms for the mapping of environmental radiation, usually by creating a 3D model of an environment and overlaying a radiation field map on top. [3, 4, 6, 7, 8, 9, 10]. However, unlike mapping radiation fields, mapping contamination involves the precise estimation of each hotspot's location and activity, which in turn affects the estimation of all other hotspots. The ability to precisely map contamination is necessary for drawing a detailed radiation distribution map [9] as well as for efficient and successful decommissioning [11].

A number of contributions have been made to the topic of contamination mapping, including those in [12-17]. The methods used in these studies are maximum likelihood estimation in [14, 15, 17], and numerical adjoints used in a Bayesian formulation in [13]. In the cases described above, either the methods are capable of locating only a single source in the environment (utilizing the inverse square law) or have a limited degree of accuracy in estimating the location of sources, especially as the number of sources and the dimension of the search space increases.

One attempt has been made to map contamination using a Particle Filter (PF) [18]. Using sparse measurements from a Geiger-Müller detector, Gao et al. localize two radiation sources in a mixed multi-modal radiation field. Although the authors note this limitation of the computationally intensive PF to operate in areas with high complexity in the paper, their limited field experiment does not demonstrate the ability to map such areas. In order to successfully apply a PF to a high-dimensional system, additional information is necessary for limiting the size of the search space. To fill this gap in the literature, our goal in the present study was to develop and test a novel algorithm that generates a contamination map of multiple point sources located on the ground. To test this algorithm, a simulator of a ground

mobile robot moving in 2D space equipped with a directional detector implemented and experimental scenarios are simulated. Our aim is to show that our algorithm is able to localize multiple sources in space quickly and accurately.

II. MATERIALS AND METHODS

This section describes the software modules of the system, which include data filtering, identification of search areas, and localization of sources using a particle filter. A search area is generated based on the filtered data, and the particle filter algorithm is then used to generate a set of particles for which there is a single source of radiation in each suspected area as well as a background source that estimates the background during the experiment.

A. Search area identification

We developed an algorithm to identify suspected contaminated areas that may contain radioactive sources in order to constrain the search space. As the mapping becomes more complex in terms of the number of sources, the size of the area and the number of visited locations, decreasing the search space greatly reduces the run time of the particle filter. There are four steps involved in the identification of an area.

Initially, the direction of the highest activity source is extrapolated up to a preset distance for each location visited by the robot. The cutoff threshold distance ensures that we do not identify false hotspots (false positives), as well as that we do not miss any sources (false negatives). Once the intersection points between the measurement lines have been calculated, they are given a weight according to the total count measurement at each location and the distance between it and the intersection point. The weight is calculated using formula (1).

$$wt = \sigma_0 \frac{d_1 d_2}{d_1 \sqrt{C_2} + d_2 \sqrt{C_1}} \quad (1)$$

Where σ_0 is the statistical sensor noise constant independent of the measurement which does not affect the *relative* quality of the intersections, d_1 and d_2 are the distances between the intersection point and the two origins of the directional measurement, and C_1 and C_2 are the total counts measured at each origin. This calculation of the weight ensures the prioritization of measurements near high activity radioactive sources, which are highly reliable. In addition, far away readings or readings pointing to low-activity sources are filtered, so this parameter should be adjusted to suit the specific environment. The intersection points are filtered so that only those with high weights remain.

Thirdly, a search area is created around each cluster of the filtered intersection points. A KMeans clustering algorithm is used to locate clusters. This clustering depends on the accuracy of the detector direction and on other noises in the measurements, and works best when there are a large number of data points compared to the number of sources. A general rule of thumb is to use half the number of measurements as the number of clusters to look for in an

environment where the number of sources is unknown.

In the final step, the multiple areas found for each cluster of intersections are combined into the final search areas that are input into the particle filter algorithm. First, area quality factors are applied to these areas, which are based on the weights of the intersections comprising them, as well as variance and distance between their points. These quality factors are then translated into changes in the size of the areas, with high quality areas being shrunk and low quality areas being enlarged. Afterwards, the filtered areas are grouped according to the overlap of the resized areas.

B. Source localization using a particle filter

The particle filter is a powerful tool for estimating the state of a system based on noisy measurements. It works by generating a set of particles, each representing a possible state of the system. These particles are then propagated through time using a model of the system dynamics and updated based on measurements taken at various times. The result is an estimate of the state of the system that is more accurate than what would be obtained by using only the measurements themselves. This approach is particularly useful in situations where direct measurement of the source is difficult, as is our case of mutual interference.

The scheme by which the particle filter operates can be seen in Fig. 1.

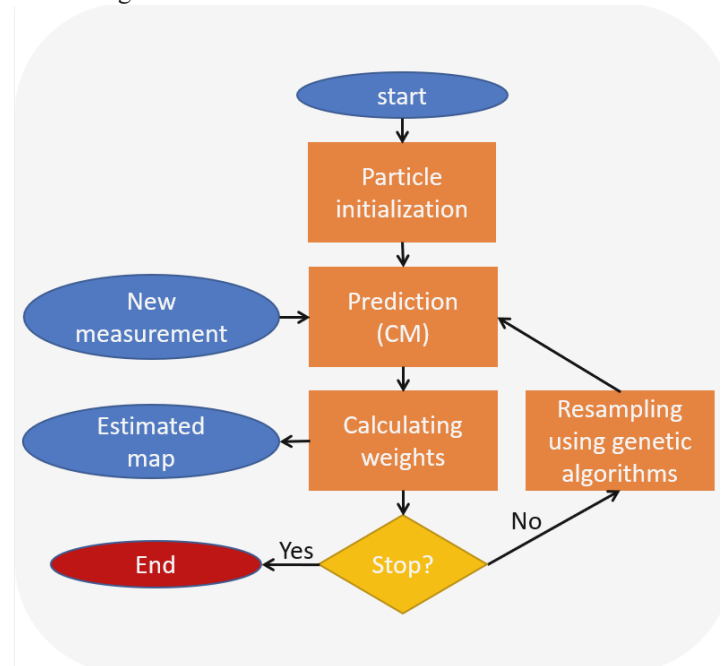


Fig. 1. Flow chart describing the particle filter algorithm

To locate the sources using the particle filter, a four-stage process is performed.

- 1) An initial set of guesses (particles) is generated. Each particle is composed of a set of sources (one for each search area), each of which has an activity level and a location on the map
- 2) For each particle, the expected readings in the locations visited by the robot are compared to the acquired readings. The expectations are calculated using the calibration matrix of the detector. The particle is given a weight based on the match to the true measurements.
- 3) Only the top 50% of particles move on to the next generation, using genetic algorithms.
- 4) A stop criterion is defined by the weight of the solutions or after a stagnation of 50 generations.

Depending on the selected percentage of particles that move onto the next generation, the algorithm will take longer converge and will be more dependent on the initial guess. Using this parameter, along with the probability and extent of mutations in the particle values, allows us to avoid local minima in exchange for run time, and to prioritize exploration over exploitation.

C. Data acquisition

For all simulations, a robot enters a suspected contaminated environment and begins collecting measurements in the area. The measurements include the total counts of the radiation field reading, and the direction of the radioactive sources in the area, weighted by their activities and distances to the detector. After saving the data of the location and the radiation field measurements, the robot moves to the next measurement point. The process is repeated until the area has been sufficiently explored.

D. Experimental setup

We simulated a total of four experimental scenarios. All locations are in meters, and the activity levels are in mCi units. Measurements had added noise levels emulating the Poisson nature of the measurement.

- 1) *Experiment 1: two sources* - In the first scenario, 16 robot measurements are simulated for an environment with two radioactive sources located 8 meters apart.
- 2) *Experiment 2: two dense sources* - In the second scenario, 16 robot measurements are simulated for an environment with two radioactive sources located 4 meters apart
- 3) *Experiment 3: two extremely dense sources* - In the third scenario, 16 robot measurements are simulated for an environment with two radioactive sources located 2 meters apart.
- 4) *Experiment 4: three sources* - In the fourth scenario, 40 robot measurements are simulated for an environment with three radioactive sources located 8 meters apart.

III. RESULTS

The purpose of this section is to describe and visualize the four experimental scenarios, together with the calculated source locations and activities as well as the ground-truth sources and activities. All simulations used 100 particles per generation, a stagnation end condition of 50 iterations without progress, and a measurement time of 10 seconds per location. The supplementary materials provide detailed information regarding the other parameters used.

In the experiment visualization plots, the purple triangles represent the robot's location, and the small angle of the

triangle indicates the direction in which the robot is oriented. At each visited location, the numbers represent the total count measurement received by the detectors. The arrows at each location indicate the direction of the weighted radiation field readings, and the weights are calculated based on the source activities and distances from the measurement site. The color of these arrows indicates the strength of the radiation field measurement in relation to the other measurements in the experiment, ranging from the lowest (white/light yellow) to the highest (black/dark red). Red stars indicate ground truth sources, and green pluses indicate sources localized by the algorithm.

Experiment 1: two sources

The visualization of Experiment 1 can be seen in Fig. 2. Although certain directional measurements in this experiment indicated uninformative orientations, the search areas were successfully identified. Both radioactive sources were located at a mean distance of 0.7 meters from the ground truth source in 61 iterations. Source activities were calculated to be 20% below ground truth activities. An explanation for this can be found in the estimated background radiation levels of $1.7 \frac{\text{counts}}{s}$ (cps) in a simulation without background radiation.

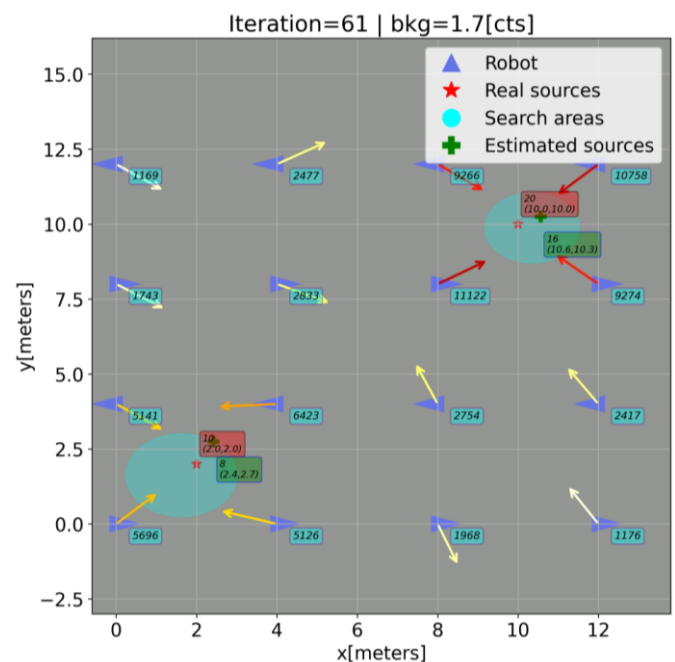


Fig. 2. Visualization of the Experiment 1 results. The ground-truth sources are $x_{1,GT}, y_{1,GT}, A_{1,GT} = (2, 2, 10)$ and $x_{2,GT}, y_{2,GT}, A_{2,GT} = (10, 10, 20)$. After reaching convergence at 61 iterations, the estimated sources are $x_{1,est}, y_{1,est}, A_{1,est} = (2.4, 2.7, 8)$ and $x_{2,est}, y_{2,est}, A_{2,est} = (10.6, 10.3, 16)$, with a calculated background radiation of 1.7 cps.

A. Experiment 2: two dense sources

The visualization of Experiment 2 can be seen in Fig. 3. Search areas are calculated correctly even when sources are four meters apart. The source with the higher activity was localized precisely, while the source with the lower activity was localized with an error of 1.6 meters. The higher level of symmetry in the data may have contributed to the longer convergence time of 103 iterations relative to Experiment 1,

since the symmetry allows for a larger number of solutions to the problem and hence increases the search space. The source activities were calculated to be 10-20% lower than the ground truth activities.

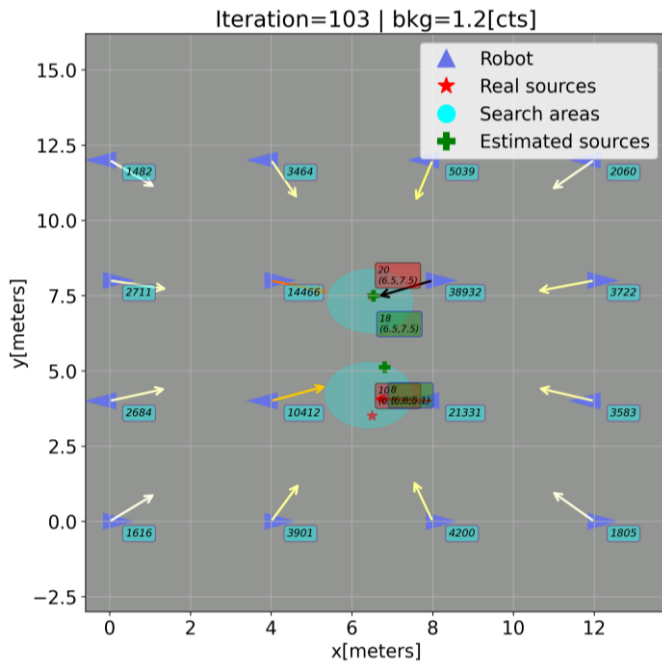


Fig. 3. Visualization of the Experiment 2 results. The ground-truth sources are $x_{1,GT}, y_{1,GT}, A_{1,GT} = (6.5, 3.5, 10)$ and $x_{2,GT}, y_{2,GT}, A_{2,GT} = (6.5, 7.5, 20)$. After reaching convergence at 103 iterations, the estimated sources are $x_{1,est}, y_{1,est}, A_{1,est} = (6.8, 5.1, 8)$ and $x_{2,est}, y_{2,est}, A_{2,est} = (6.5, 7.5, 18)$, with a calculated background radiation of 1.2 cps.

B. Experiment 3: two extremely dense sources

The visualization of Experiment 3 can be seen in Fig. 4. At a distance of 2 meters between the sources, the algorithm finds only one search area containing a single source, and the average error in localization is 1 meters. The source's equivalent activity level was calculated to be less than 20% below the sum of the ground truth activities in only 41 iterations, which can be attributed to the low complexity of the search space.

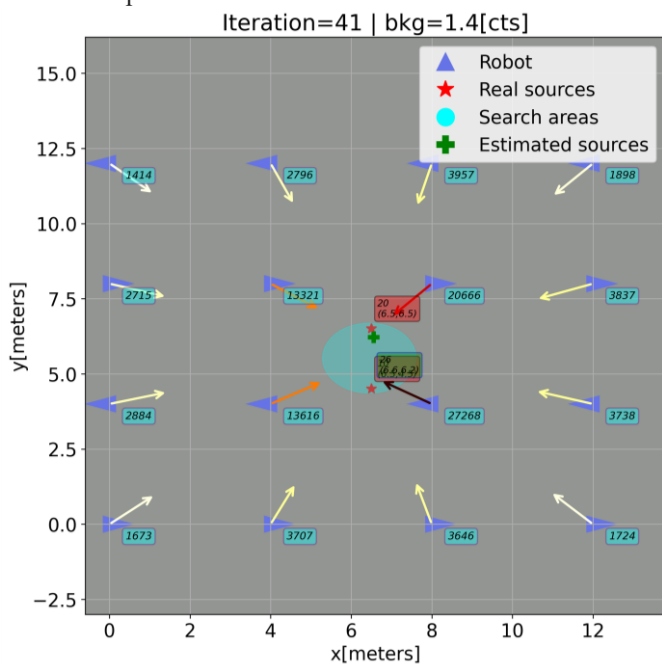


Fig. 4. Visualization of the Experiment 3 results. The ground-truth sources

are $x_{1,GT}, y_{1,GT}, A_{1,GT} = (6.5, 4.5, 10)$ and $x_{2,GT}, y_{2,GT}, A_{2,GT} = (6.5, 6.5, 20)$. After reaching convergence at 41 iterations, the estimated source is $x_{1,est}, y_{1,est}, A_{1,est} = (6.6, 6.2, 26)$ which appears to be an average of the two ground truth sources, with a calculated background radiation of 1.4 cps.

C. Experiment 4: three sources

The visualization of Experiment 4 can be seen in Fig. 5. The algorithm detected all three radioactive sources and located them near their respective ground truth sources, with an average localization error of 1 meter. The source activities were calculated to be 20-30% lower than the ground truth activities, since the calculated background level was high.

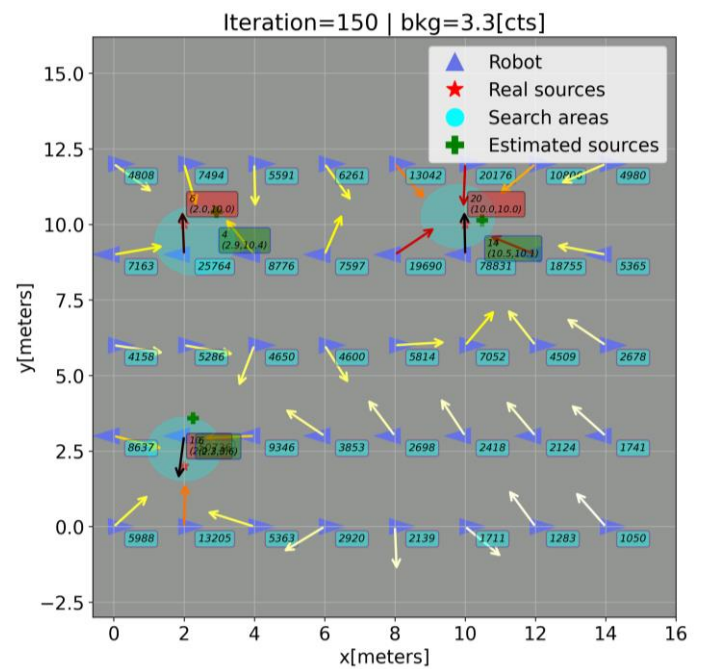


Fig. 5. Visualization of the Experiment 4 results. The ground-truth sources are $x_{1,GT}, y_{1,GT}, A_{1,GT} = (2, 2, 10)$, $x_{2,GT}, y_{2,GT}, A_{2,GT} = (10, 10, 20)$ and $x_{3,GT}, y_{3,GT}, A_{3,GT} = (2, 10, 6)$. After reaching convergence at 150 iterations, the estimated sources are $x_{1,est}, y_{1,est}, A_{1,est} = (2.3, 3.6, 6)$, $x_{2,est}, y_{2,est}, A_{2,est} = (10.5, 10.1, 14)$ and $x_{3,est}, y_{3,est}, A_{3,est} = (2.9, 10.4, 4)$, with a calculated background radiation of 3.3 cps.

The simulation results for all four scenarios are presented in Table I.

TABLE I
TRENDS IN LOCALIZATION AND SOURCE ACTIVITIES ERRORS.

Experiment name	Average Localization error (meters)	Average activity value error (% of ground truth value)	Estimated background radiation (cps)
Two sources	0.73 ± 0.01	20 ± 0.1	1.7 ± 0.1
Two dense sources	0.81 ± 0.01	15 ± 0.1	1.2 ± 0.1
Two extremely dense sources	1.00 ± 0.01	32.5 ± 0.1	1.4 ± 0.1
Three sources	1.04 ± 0.01	34.4 ± 0.1	3.3 ± 0.1

As the experiments became more complex, the localization and activity level errors increased. We also notice a correlation between the estimated background and the error in the activity values for experiments 1, 2 and 4.

IV. DISCUSSION

In this study, we present a novel algorithm for multi-source contamination mapping using a simulation of a mobile robot equipped with a directional detector. The research aimed to improve contamination mapping and decommissioning processes by accurately locating and estimating the activities of multiple point radioactive sources on the ground.

Simulated experiments demonstrated the effectiveness of the proposed algorithm. In Experiments 1, 2 and 4, the algorithm successfully detected the number of contamination sources on the map, demonstrating its effectiveness of the search area identification. In Experiment 3, a distance of 2 meters proved too little for the algorithm to differentiate between the sources. A possible solution for this is to improve the area clustering algorithm to allow for smarter clustering and noticing subtle subgroups of clusters.

The algorithm was successful in localizing the sources within 0.9 meters of the ground truth locations on average. Additionally, the algorithm achieved an accuracy of 25.5% for activity level, which can be attributed to the estimated background. Because there was no simulated background radiation, any calculated background level will decrease the levels of source activity to create a good fit to the data. This tradeoff is evident in the correlation between the level of background radiation and the percentage of activity level inaccuracy for experiments 1, 2 and 4. The average runtime of each iteration was 4 seconds, resulting in a mean runtime of 6 minutes for each simulation. These findings indicate the algorithm's potential for real-world applications, in which these values could be used to plan a mission for collecting data near the sources, thus improving localization and facilitating further steps.

Small improvements in localization are likely to lead to greater improvements since an error in localization for one source is often compensated by an increased error in another source's location if the resulting source set creates a radiation field which better fits the data.

The particle filter was a central component of the algorithm, enabling the estimation of hotspot locations and activities based on noisy measurements. The use of the directional readings provided crucial information about the direction of the sources, which enabled the calculation of search areas and reduced the parameter search space of the particle filter. By incorporating directional information into the algorithm, it greatly improved its performance and contributed to its practical application in real-world settings.

Despite the success of the proposed algorithm, there are some limitations and challenges that need to be addressed. A number of improvements are planned for the area clustering algorithm in the future, as well as extensive testing of the algorithm. Secondly, source differencing techniques can increase the accuracy of the resulting map. Thirdly, it is important to note that the performance of the algorithm is influenced by parameter choices, such as the threshold for intersections and the method for grouping the search areas. Finding the optimal parameter values for specific scenarios requires careful consideration.

We expect that an updated version of the directional measurements which points to the strongest point source in the area would greatly improve the results. With the

implementation of these suggestions, the algorithm presented in this paper, could provide a robust response to radioactive contamination incidents on-site, where rapid area contamination mapping is critical and human safety is of paramount importance.

V. CONCLUSION

In this study, we developed an algorithm for efficient and accurate multi-source contamination mapping using a mobile robot equipped with a directional detector. The combination of directional measurements and particle filter-based source localization allowed for successful mapping of multiple point sources located on the ground. Provided sufficient testing and the development of a physical setup, this system could be quickly deployed in response to radioactive contamination incidents to ensure quick area contamination mapping while prioritizing human safety. Future research should focus testing more scenarios with various densities and activity levels, improving the area clustering algorithm and improving the mission planning for online applications in order to provide a more accurate map and greater applicability in real-world scenarios.

REFERENCES

- [1] F. Mascarich, T. Wilson, C. Papachristos, and K. Alexis, "Radiation Source Localization in GPS-Denied Environments Using Aerial Robots," in 2018 IEEE International Conference on Robotics and Automation (ICRA), Brisbane, QLD: IEEE, May 2018, pp. 6537–6544. doi: 10.1109/ICRA.2018.8460760.
- [2] I. Tsitsimpelis, C. J. Taylor, B. Lennox, and M. J. Joyce, "A review of ground-based robotic systems for the characterization of nuclear environments," *Progress in Nuclear Energy*, vol. 111, pp. 109–124, Mar. 2019, doi: 10.1016/j.pnucene.2018.10.023.
- [3] B. Bird et al., "A Robot to Monitor Nuclear Facilities: Using Autonomous Radiation-Monitoring Assistance to Reduce Risk and Cost," *IEEE Robot. Automat. Mag.*, vol. 26, no. 1, pp. 35–43, Mar. 2019, doi: 10.1109/MRA.2018.2879755.
- [4] S. R. White et al., "Radiation Mapping and Laser Profiling Using a Robotic Manipulator," *Front. Robot. AI*, vol. 7, p. 499056, Nov. 2020, doi: 10.3389/frobt.2020.499056.
- [5] P. G. Martin et al., "3D unmanned aerial vehicle radiation mapping for assessing contaminant distribution and mobility," *International Journal of Applied Earth Observation and Geoinformation*, vol. 52, pp. 12–19, Oct. 2016, doi: 10.1016/j.jag.2016.05.007.
- [6] Martin, Peter G. & Scott, Thomas & Payton, Oliver & Fardoulis, John. (2017). High-Resolution Aerial Radiation Mapping for Nuclear Decontamination and Decommissioning.
- [7] P. Martin, J. Moore, J. Fardoulis, O. Payton, and T. Scott, "Radiological Assessment on Interest Areas on the Sellafield Nuclear Site via Unmanned Aerial Vehicle," *Remote Sensing*, vol. 8, no. 11, p. 913, Nov. 2016, doi: 10.3390/rs8110913.
- [8] Abd. H. Zakaria, Y. M. Mustafah, J. Abdullah, N. Khair, and T. Abdullah, "Development of Autonomous Radiation Mapping Robot," *Procedia Computer Science*, vol. 105, pp. 81–86, 2017, doi: 10.1016/j.procs.2017.01.203.
- [9] Y. Sato et al., "Radiation imaging using a compact Compton camera inside the Fukushima Daiichi Nuclear Power Station building," *Journal of Nuclear Science and Technology*, vol. 55, no. 9, pp. 965–970, Sep. 2018, doi: 10.1080/00223131.2018.1473171.
- [10] K. Vetter, R. Barnowski, A. Haefner, T. H. Y. Joshi, R. Pavlovsky, and B. J. Quiter, "Gamma-Ray imaging for nuclear security and safety: Towards 3-D gamma-ray vision," *Nuclear Instruments and Methods in Physics Research Section A: Accelerators, Spectrometers, Detectors and Associated Equipment*, vol. 878, pp. 159–168, Jan. 2018, doi: 10.1016/j.nima.2017.08.040.
- [11] Y. Sato, Y. Terasaka, S. Ozawa, Y. Tanifuji, and T. Torii, "A 3D radiation image display on a simple virtual reality system created using a game development platform," *J. Inst.*, vol. 13, no. 08, pp. T08011–T08011, Aug. 2018, doi: 10.1088/1748-0221/13/08/T08011.
- [12] T. Baca et al., "Gamma Radiation Source Localization for Micro Aerial Vehicles with a Miniature Single-Detector Compton Event Camera," in 2021 International Conference on Unmanned Aircraft

- Systems (ICUAS), Athens, Greece: IEEE, Jun. 2021, pp. 338–346. doi: 10.1109/ICUAS51884.2021.9476766.
- [13] K. D. Jarman, E. A. Miller, R. S. Wittman, and C. J. Gesh, “Bayesian Radiation Source Localization,” *Nuclear Technology*, vol. 175, no. 1, pp. 326–334, Jul. 2011, doi: 10.13182/NT10-72.
- [14] H. Wan, T. Zhang, and Y. Zhu, “Detection and localization of hidden radioactive sources with spatial statistical method,” *Ann Oper Res*, vol. 192, no. 1, pp. 87–104, Jan. 2012, doi: 10.1007/s10479-010-0805-z.
- [15] H. E. Baidoo-Williams, “Maximum Likelihood Localization of Radiation Sources with unknown Source Intensity,” arXiv, Oct. 10, 2016. Accessed: Aug. 02, 2023. [Online]. Available: <http://arxiv.org/abs/1608.00427>
- [16] H. E. Baidoo-Williams, R. Mudumbai, E. Bai, and S. Dasgupta, “Some theoretical limits on nuclear source localization and tracking,” in *2015 Information Theory and Applications Workshop (ITA)*, San Diego, CA, USA: IEEE, Feb. 2015, pp. 270–274. doi: 10.1109/ITA.2015.7309000.
- [17] G. Cordone et al., “Improved multi-resolution method for MLE-based localization of radiation sources,” in *2017 20th International Conference on Information Fusion (Fusion)*, Xi’an, China: IEEE, Jul. 2017, pp. 1–8. doi: 10.23919/ICIF.2017.8009626.
- [18] W. Gao, W. Wang, H. Zhu, G. Huang, D. Wu, and Z. Du, “Robust Radiation Sources Localization Based on the Peak Suppressed Particle Filter for Mixed Multi-Modal Environments,” *Sensors*, vol. 18, no. 11, p. 3784, Nov. 2018, doi: 10.3390/s18113784.